Journal of Alloys and Compounds 478 (2009) 427–436

Contents lists available at ScienceDirect

Journal of Alloys and Compounds

journal homepage: www.elsevier.com/locate/jallcom

Experimental study of the Ce–Mg–Zn phase diagram at 350 °C via diffusion couple techniques

D. Kevorkov, M. Pekguleryuz*

McGill University, Mining and Materials Engineering, 3600 University Street, Montreal, Quebec, Canada

ARTICLE INFO

Article history:
Received 30 August 2008
Received in revised form 5 November 2008
Accepted 10 November 2008
Available online 3 December 2008

Keywords:
Metals and alloys
Phase diagrams
Diffusion
Scanning electron microscopy (SEM)

ABSTRACT

Ce modification of commercial AZ alloys has great potential for the development of Mg alloys with improved formability and creep resistance. Because the solid solubility of Ce in (Mg) solid solution is extremely low, the precipitation of Ce containing intermetallics is expected even at low Ce concentrations. The Ce–Mg–Zn phase diagram at 350 °C was studied in this work by means of diffusion couple techniques. Precipitation of intermetallic phases in the Mg-rich corner has been analyzed using Scanning electron microscopy (SEM) and their compositions were determined by energy dispersive spectroscopy (EDS).

1. Introduction

The Ce–Mg–Zn ternary system is a key system for the development Ce and Zn containing multicomponent alloys. Ce additions to commercial AZ alloys have the potential to modify the microstructure and improve the formability or creep resistance of Mg alloys. Because the solid solubility of Ce in (Mg) solid solution is extremely low, the precipitation of Ce containing intermetallics is expected even at low Ce concentrations. The main aim of this work was the determination of precipitates in Ce–Mg–Zn system. The study of the Mg rich corner of the Ce–Mg–Zn ternary system provides important information about phase equilibria between Mg matrix and the precipitating phases.

2. Background

2.1. Binary systems

The Ce–Mg–Zn ternary system contains three binary subsystems: Mg–Ce, Mg–Zn and Ce–Zn. Because the knowledge of binary phase equilibria is important for the understanding of ternary equilibria, a brief overview of the binary phase diagrams is presented below.

2.1.1. Mg–Ce system

Mg–Ce phase diagram presented in Fig. 1 is redrawn from Massalski et al. [1]. It contains six intermetallic compounds. Only four of those are stable at 350 °C. Mg–Ce binary phase diagram was studied in the whole range of concentrations, but the compositions of intermetallic phases and their homogeneity ranges have not been determined exactly. The solid solution ranges of $Mg_{12}Ce$ and Mg_3Ce compounds are plotted in dotted lines on the phase diagram (Fig. 1). The compositions of intermetallic phases from the latest work of Zhang et al. [2], who studied phase equilibria at 400 °C via the diffusion couple technique, do not correspond to the ones from the assessment in Massalski handbook [1].

The phase compositions extracted from [1] and [2] are presented in Table 1. The original results of the Electron Probe Micro Analysis (EPMA) of interdiffusion layers published in [2] were averaged from ten measurements for each phase and unfortunately not normalized to 100%. Therefore, they were recalculated in the present study in order to compare to the values of Massalski and co-workers [1].

2.1.2. Mg–Zn system

Two literature reviews on Mg–Zn system have been found in the literature. The recent one, shown in Fig. 2, has been published by Predel [3], but the phase diagram is mainly based on the previous assessment of Clark et al. [4] (Fig. 3). The assessment of Predel [3] contains additional information on metastable equilibria in the Zn-rich region as well as an extensive review of the thermodynamic data. The phase diagram contains five intermetallic phases. All of

* Corresponding author.
E-mail address: mihriban.pekguleryuz@mcgill.ca (M. Pekguleryuz).

0925-8388/$ – see front matter © 2008 Elsevier B.V. All rights reserved.
doi:10.1016/j.jallcom.2008.11.119

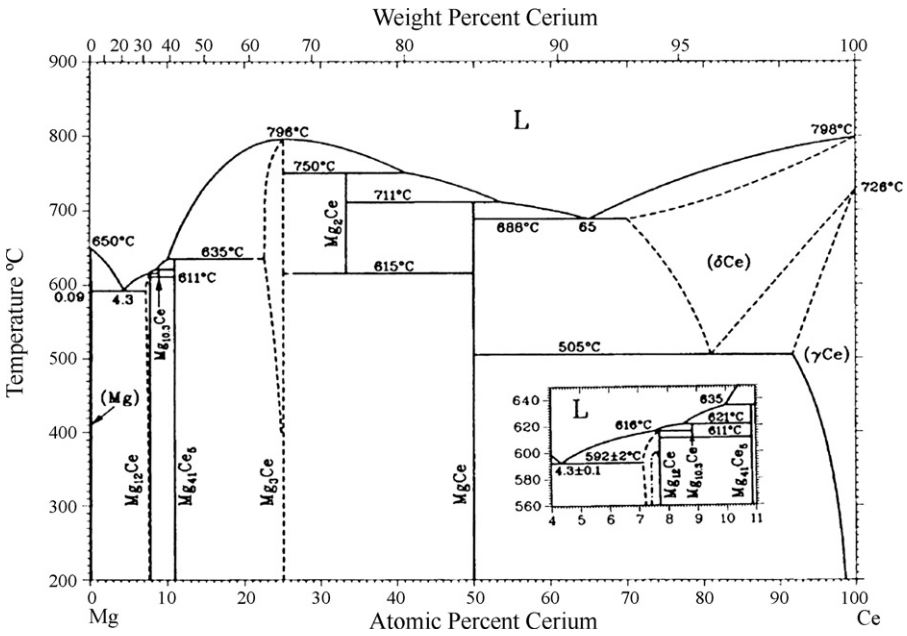

Fig. 1. Mg–Ce binary phase diagram (redrawn from Massalski et al. [1]).

Table 1
Phase compositions of low temperature intermetallic phases (extracted from [1] and [2]).

Phase	Phase compositions [1]		EPMA measurements [2]		Recalculated values of ref. [2]	
	Mg (at%)	Ce (at%)	Mg (at%)	Ce (at%)	Mg (at%)	Ce(at%)
$Mg_{12}Ce$	92.31	7.69	90.10	8.36	91.51	8.49
$Mg_{41}Ce_5$	89.13	10.87	87.56	11.39	88.49	11.51
Mg_3Ce	? to 75	? to 25	73.24	24.68	74.80	25.20
MgCe	50	50	46.57	48.88	48.79	51.21

them have narrow homogeneity ranges, but since they are marked as dashed lines on the phase diagrams illustrated in Figs. 2 and 3, it can be concluded that the exact phase boundaries have not been determined.

2.1.3. Ce–Zn system

The Ce–Zn phase diagram presented in Fig. 4 is redrawn from the Massalski et al. [5]. This system contains nine stoichiometric phases. All phases have high temperatures of formation. Therefore,

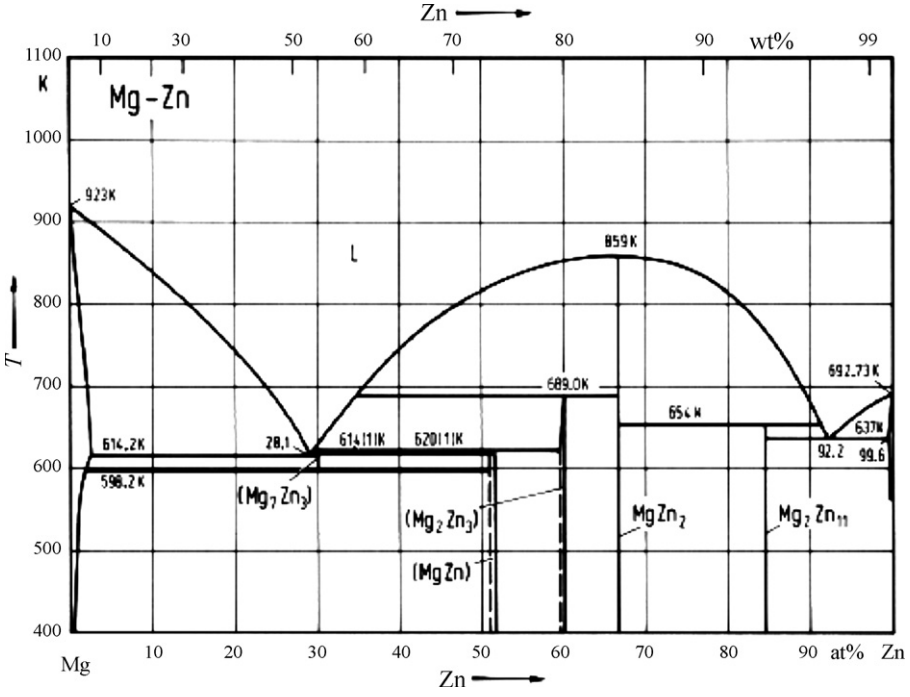

Fig. 2. Mg–Zn binary phase diagram (redrawn from [3]).

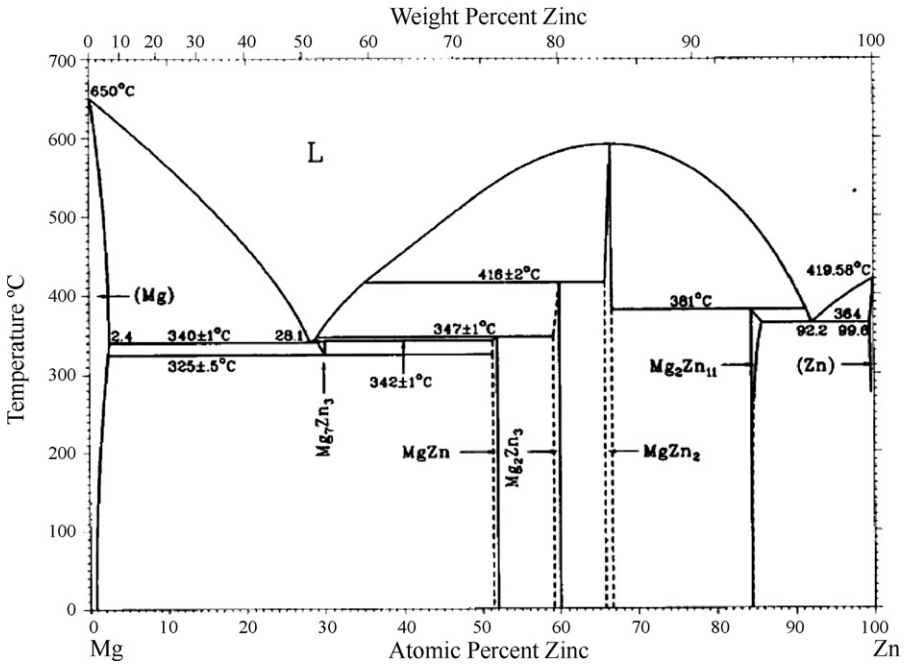

Fig. 3. Mg–Zn binary phase diagram (redrawn from [4]).

they can potentially precipitate or exist in the ternary Ce–Mg–Zn phase equilibria.

2.2. Ternary Mg–Ce–Zn system

The literature review on Ce–Mg–Zn system was prepared by Kolitsch et al. [6]. The system was first studied in the region between 0 and 80 mass% Mg by Korolkov and Saldau [7]. Thermal analysis was used to construct six vertical sections with a constant mass ratio Zn:Ce of 1:5, 1:2, 1:1, 2:1, 4.5:1 and 10:1, and a liquidus surface of the Mg corner was drawn. Several authors [8–10] studied the phase relations in the Mg-rich corner of the Ce–Mg–Zn ternary system. Phase triangulation in the region Mg–$MgZn_2$–CeMg–CeZn has been evaluated by means of X-ray powder diffraction [9] from 150 alloys annealed at 300 °C for 240 h and quenched in water. Four ternary compounds were observed by Melnik et al. [9]. Drits et al. [10] constructed two polythermal sections in the Mg-rich corner at 24 mass% Zn and 34 mass% Zn, both ranging from 0 to 20 mass% Ce. The DTA (cooling rates 2–5 K/min), electron probe microanalysis (EPMA), scanning electron microscopy (SEM) and X-ray powder diffraction were used for the construction of polythermal sections. No recent experimental studies were found on this ternary system.

The partial isothermal section presented in Fig. 5 was assessed by Kolitsch et al. [6] taking into account all previous data. Since the

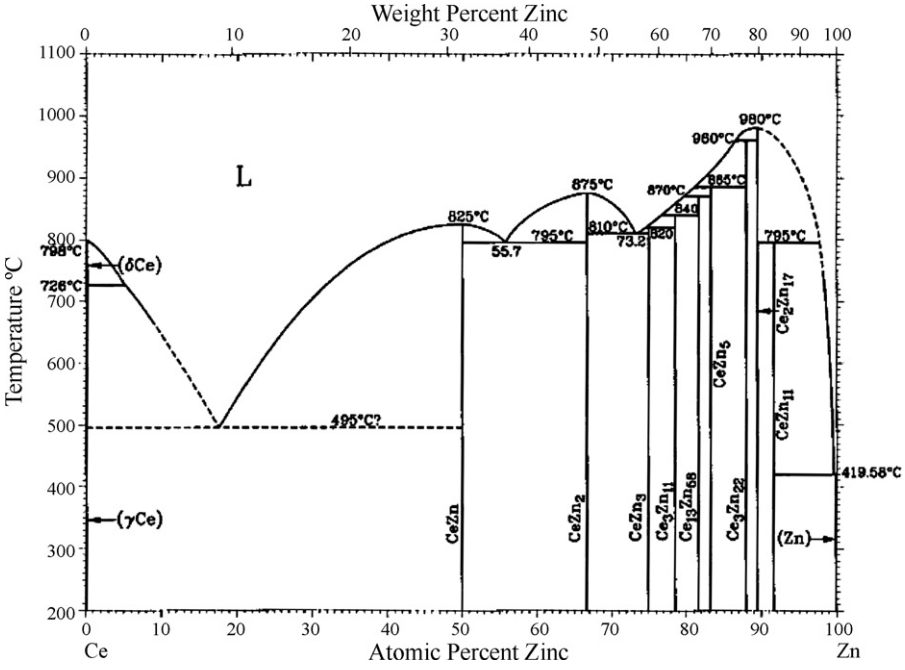

Fig. 4. Ce–Zn binary phase diagram (redrawn from [4]).

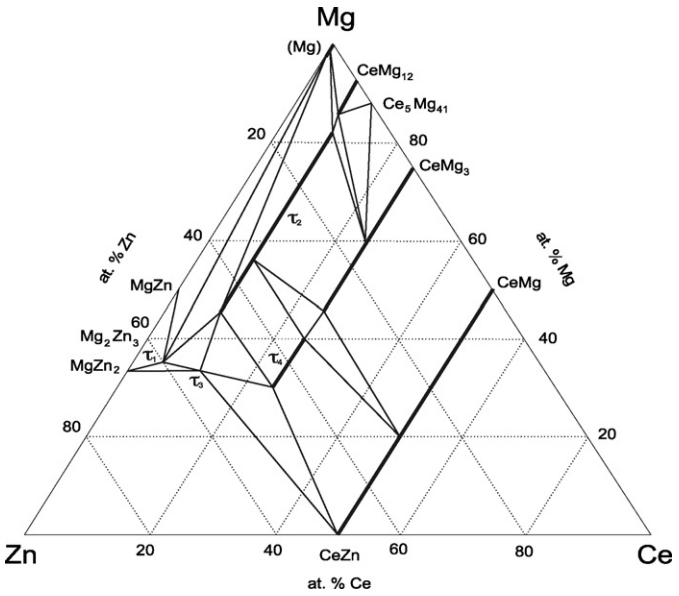

Fig. 5. Partial isothermal section at 300 °C.

present study aimed an analysis of the isothermal section at 350 °C, the most interesting data for this paper is the partial isothermal section at 300 °C.

3. Experimental procedure

In order to study phase relations in Mg-rich corner of Ce–Mg–Zn system, five diffusion couples were prepared and studied by SEM/energy dispersive spectroscopy (EDS), FEGSEM/EDS and EPMA. Pure elements were used for sample preparation: Mg ingots with the purity of 99.98% supplied by Timminco, and Ce 99.7% supplied by Hefa and Zn 99.99% supplied by Alfa Aesar.

3.1. Solid–solid diffusion couples

Three solid–solid diffusion couples were prepared and annealed at 350 °C for 16 days. Their compositions are:

- {Mg–4 at% Zn}–Ce
- {Mg–50 at% Zn}–Ce
- {Mg–54 at% Zn}–Ce.

Mg–Zn alloys were prepared in the induction furnace under CO_2–0.5% SF_6 protective gas cover. The solid–solid diffusion couples were prepared from the 10 mm × 7 mm × 7 mm blocks of pure Ce and Mg–Zn alloys. The contacting surfaces were grinded with SiC paper up to 1200 grid and polished with a diamond paste up to 1 μm. The 95 vol% alcohol was used as a lubricant. The blocks were put into intimate contact and pressurized using the steel clamping rings. The diffusion couples were packed in Ta foil, sealed in the quartz tubes in vacuum, annealed in at 350 °C for 23 days, and then quenched in liquid nitrogen. Tantalum foil was used to avoid a reaction between the alloys and the quartz.

3.2. Solid–liquid diffusion couples

Two solid–liquid diffusion couples were prepared and annealed at 350 °C for 23 days:

- {Mg–3.5 at% Ce}–Zn
- {Mg–8.5 at% Ce}–Zn

The solid–liquid diffusion couples were prepared by placing the solid alloy pieces into a liquid Zn. Mg–Ce alloys were prepared in a Lindberg Blue M electrical resistance furnace in a mild steel crucible, and CO_2–0.5% SF_6 cover gas was used to protect the melt. The 10 mm × 7 mm × 7 mm blocks of Mg–Ce alloys were grinded from all sides with SiC paper up to 1200 grid and polished with a diamond paste up to 1 μm.

The 150 g of Zn were melted at 500 °C under protective CO_2–0.5% SF_6 atmosphere in the induction furnace. Solid alloys were immersed into liquid Zn and the power of the induction furnace was immediately turned out to prevent complete dissolution of the solid alloys. The samples were cooled to the room temperature and the solid–liquid diffusion couples were cut out from the bulks for thermal treatment. The diffusion couples were annealed in the same way as the solid–solid diffusion couples. Terminal compositions of the diffusion couples are shown in Fig. 6.

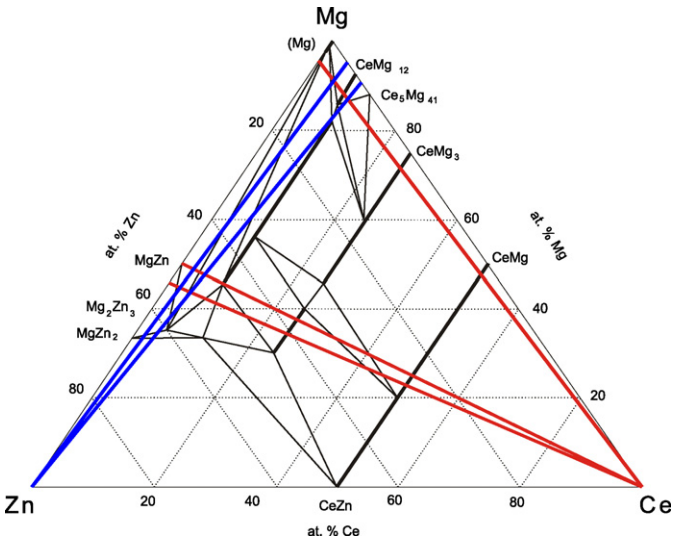

Fig. 6. Terminal compositions C_1–C_5 of the diffusion couples.

The interdiffusion zones formed after annealing were analyzed using EDS and EPMA. The diffusion paths were analyzed and the phase equilibria have been determined. Based on these results a partial ternary phase diagram was constructed.

4. Results and discussion

After careful review of the literature data, the partial isothermal section at 300 °C assessed by Kolitsch et al. [6] was taken as a starting point of the present study. Taking into account that a 50 °C difference may cause variation of the solid solubility regions, experimental results were compared to the assessment of Kolitsch et al. [6]. Numerous discrepancies between the experimental results and the assessed partial isothermal section were found. The partial isothermal section constructed in this study shows substantial deviations from the assessment of Kolitsch et al. [6]. In order to present the results of the present study, the final version of the partial phase diagram shown in Fig. 7 is utilized, so that the diffusion paths and phase equilibria that have been determined can be directly related to the phase diagram.

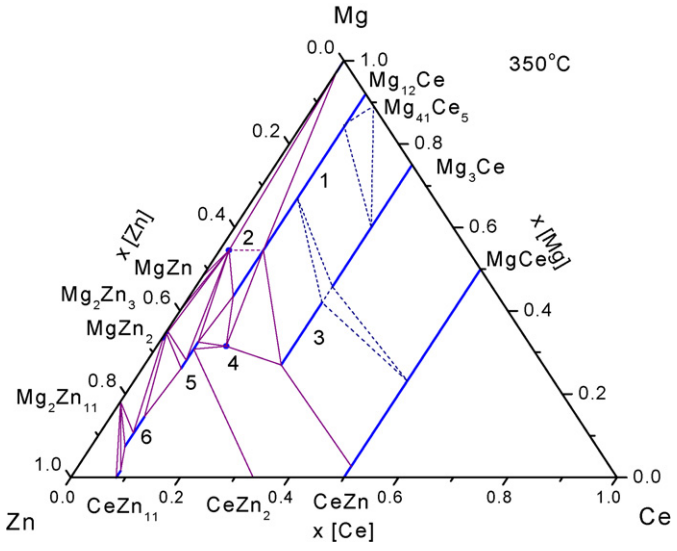

Fig. 7. Partial isothermal section at 350 °C.

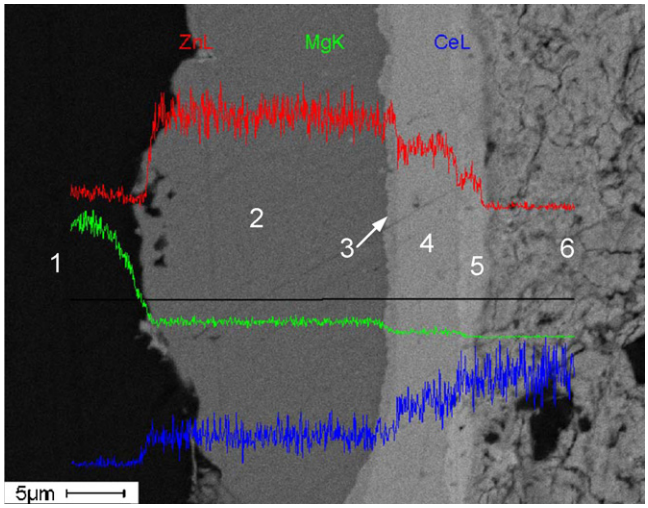

Fig. 8. SEM micrograph and line scan of the {Mg–4 at% Zn}–Ce solid–solid diffusion couple.

Table 2
Results of EDS analysis of interdiffusion layers in the {Mg–4 at% Zn}–Ce diffusion couple.

	Ce (at%)	Mg (at%)	Zn (at%)	Comments
Zone 1	0	96.03	3.97	Mg solid solution in the Mg–4 at% Zn binary alloy
Zone 2	7.8	54.7	37.5	Phase 1 (denoted as τ_2 by Kolitsch et al. [6])
Zone 3	12.7	31.5	55.8	Phase 4
Zone 4	23.6	28.1	48.3	Phase 3
Zone 5	48.0	3.6	48.4	Phase 7
Zone 6	100	0	0	Pure Ce

4.1. {Mg–4 at% Zn}–Ce solid–solid diffusion

The micrograph of {Mg–4 at% Zn}–Ce solid–solid diffusion couple at 350 °C presented in Fig. 8 contains six zones. It was studied via SEM/EDS and the results of quantitative EDS analysis are presented in Table 2. The diffusion path is shown in Fig. 9. The diffusion path starts at the Mg solid solution (zone 1), crosses $(Mg,Zn)_{12}Ce$ solid solution (denoted as τ_2 by Kolitsch et al. [6] and marked as Phase 1 on Fig. 9) and goes to the Phase 4.

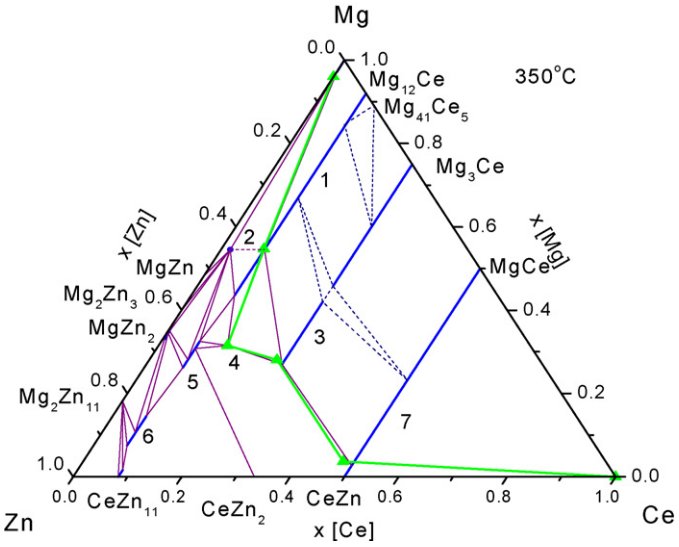

Fig. 9. {Mg–4 at% Zn}–Ce diffusion path.

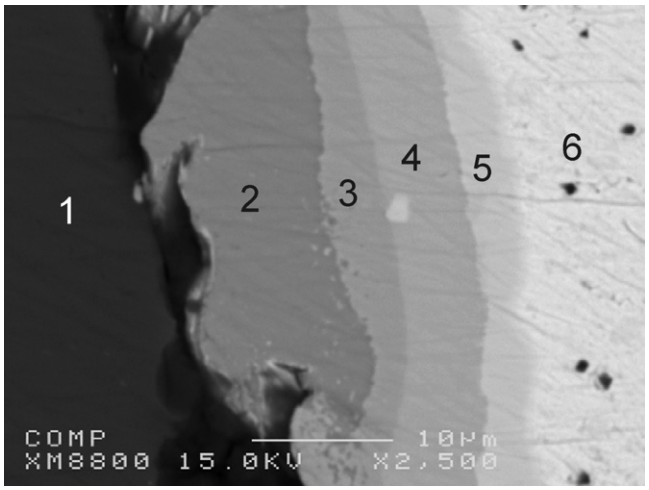

Fig. 10. {Mg–4 at% Zn}–Ce solid–solid diffusion couple. Six interdiffusion layers, region #1.

It is believed that Phase 4 corresponds to the τ_3 phase reported by Kolitsch et al. [6], but the composition is slightly shifted. From Phase 4 the diffusion path goes to Phase 3 (denoted by τ_4 as shown by Kolitsch et al. [6]) and it can be deducted that the composition presented in Table 2 corresponds or is very close to the maximal solid solubility of this solid solution. The reason for such a statement is that the following diffusion path crosses the (Mg,Zn)Ce solid solution near the pure CeZn composition. This means that the composition of Phase 3 should be very close to the composition of the ternary equilibria and to the maximal solid solubility of the solid solution. From the (Mg,Zn)Ce solid solution (zone 5) the diffusion path goes to the pure Ce (zone 6).

Careful analysis of the other regions in the interdiffusion zone shows some compositional fluctuations in the interdiffusion layers. Moreover, in some regions not six but five layers were formed. The EPMA was carried out to analyze these regions. Two "6-interdiffusion" layer regions and two "5-interdiffusion" layer regions were studied by EPMA to investigate the phase equilibria between the layers. The micrographs of these regions are shown in Figs. 10–15. The results of quantitative EPMA analysis are presented in Tables 3 and 4.

Analysis of compositions in 6-interdiffusion layer regions (Table 3) demonstrated that they are close to the results of EDS

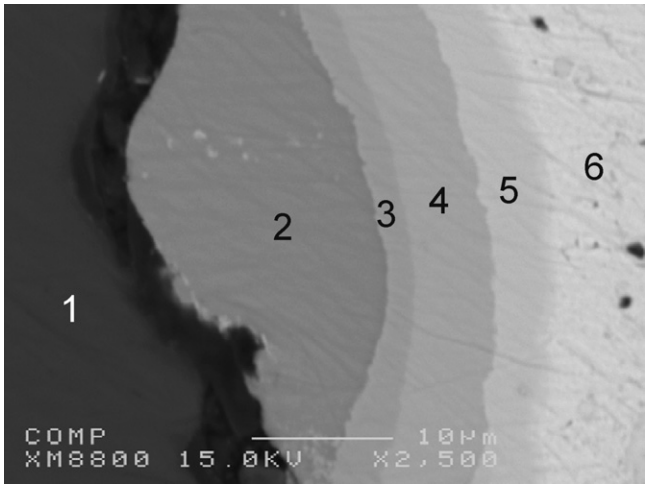

Fig. 11. {Mg–4 at% Zn}–Ce solid–solid diffusion couple. Six interdiffusion layers, region #2.

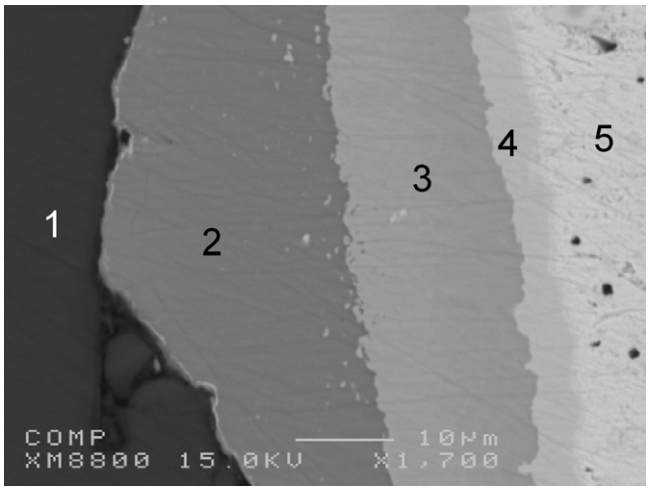

Fig. 12. {Mg–4 at% Zn}–Ce solid–solid diffusion couple. Five interdiffusion layers, region #3.

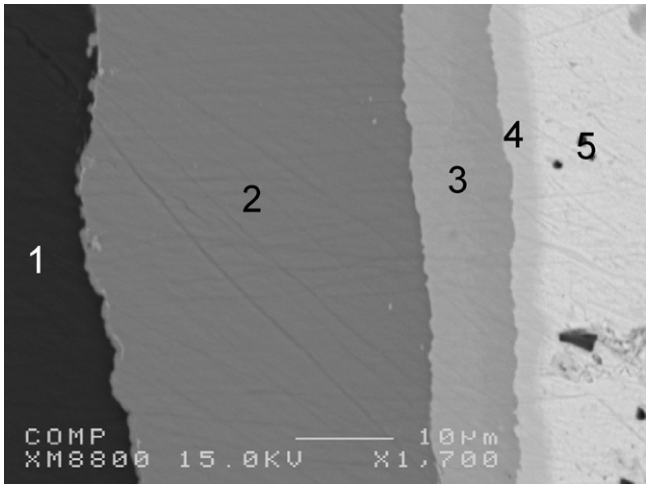

Fig. 13. {Mg–4 at% Zn}–Ce solid–solid diffusion couple. Five interdiffusion layers, region #4.

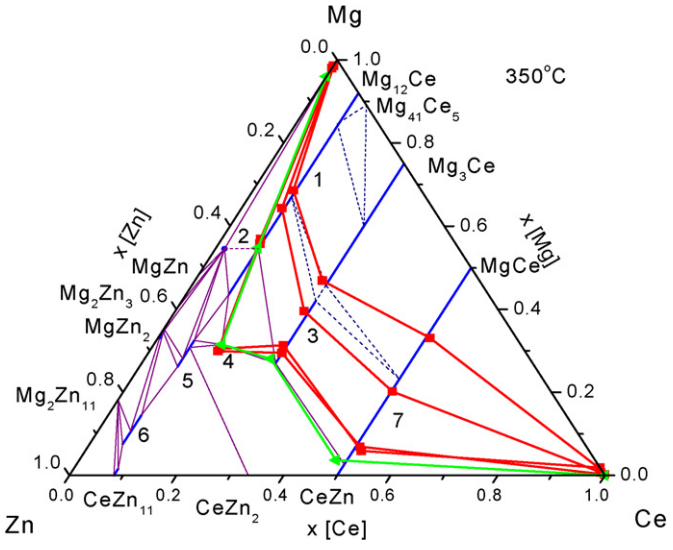

Fig. 14. {Mg–4 at% Zn}–Ce diffusion paths. Four diffusion paths analyzed by EPMA (lines with squares) and the diffusion path analyzed by EDS (line with triangles).

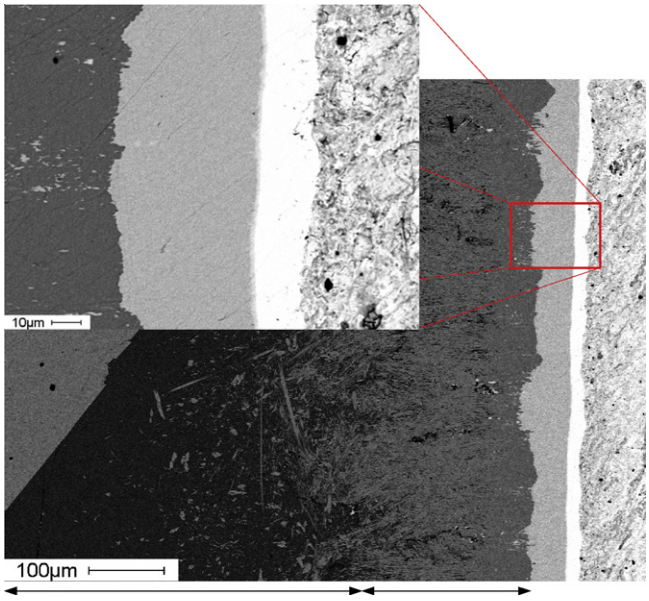

Fig. 15. {Mg–50 at% Zn}–Ce solid–solid diffusion couple.

Table 3
Results of EPMA analysis of six interdiffusion layers zone in the {Mg–4 at% Zn}–Ce diffusion couple.

	Ce (at%)	Mg (at%)	Zn (at%)	Comments
Region 1				
Layer 1	0.00	98.06	1.94	Mg solid solution in the Mg–4 at% Zn binary alloy
Layer 2	7.26	56.89	35.85	Phase 1 (denoted as τ_2 by Kolitsch et al. [6])
Layer 3	12.81	29.91	57.28	Phase 4
Layer 4	24.96	29.51	45.54	Phase 3
Layer 5	50.81	6.92	42.27	Phase 7
Layer 6	99.79	0.21	0.00	Pure Ce
Region 2				
Layer 1	0.01	98.01	1.98	Mg solid solution in the Mg–4 at% Zn binary alloy
Layer 2	7.66	55.80	36.53	Phase 1 (denoted as τ_2 by Kolitsch et al. [6])
Layer 3	12.82	30.47	56.71	Phase 4
Layer 4	24.30	31.31	44.39	Phase 3
Layer 5	51.52	5.95	42.53	Phase 7
Layer 6	98.11	1.89	0.00	Pure Ce

Table 4
Results of EPMA analysis of five interdiffusion layers zone in the {Mg–4 at% Zn}–Ce diffusion couple.

	Ce (at%)	Mg (at%)	Zn (at%)	Comments
Region 3				
Zone 1	0.01	98.68	1.30	Mg solid solution in the Mg–4 at% Zn binary alloy
Zone 2	7.55	68.64	23.82	Phase 1 (denoted as τ_2 by Kolitsch et al. [6])
Zone 3	23.79	46.89	29.32	Phase 3
Zone 4	50.79	33.10	16.11	Phase 7
Zone 5	98.27	1.61	0.12	Pure Ce
Region 4				
Zone 1	0.01	98.56	1.43	Mg solid solution in the Mg–4 at% Zn binary alloy
Zone 2	7.52	64.30	28.18	Phase 1 (denoted as τ_2 by Kolitsch et al. [6])
Zone 3	24.06	39.56	36.38	Phase 3 or $(Mg,Zn)_3Ce$ solid solution
Zone 4	50.22	20.18	29.60	Phase 7
Zone 5	98.88	0.73	0.38	Pure Ce

Table 5
Results of EDS analysis of interdiffusion layers in the {Mg–50 at% Zn}–Ce diffusion couple.

	Ce (at%)	Mg (at%)	Zn (at%)	Comments
Zone 1	0	49.88	50.12	Mg–50 at% Zn binary alloy
Zone 2	1.82	54.79	45.39	Phase 2
Zone 3	7.70	28.99	63.32	Phase 5
Zone 4	32.59	0	67.41	$CeZn_2$
Zone 5	100	0	0	Pure Ce

analyses shown in Table 2. Nevertheless, concentrations of the Phases 3 and 7 in regions 1 and 2 (Table 3) contain less Zn than these phases in the zone analyzed by EDS (Table 2). This means that phase equilibria between Phases 3 and 7 in regions 1 and 2 correspond to the tie-lines in the two-phase region "Phase 3–Phase 7".

The study of the two "5-interdiffusion layer" regions gave the two-phase equilibria data between the solid solutions. The diffusion path for region 3 is the following: (Mg)–(Phase 1)-(Phase 3)-(Phase 7)–(Ce). The diffusion path for region 4 is the following: (Mg)–(Phase 1)-$(Mg,Zn)_3Ce$-(Phase 7)–(Ce). All four diffusion paths analyzed by EPMA (lines with squares) as well as the diffusion path analyzed by EDS (line with triangles) are presented in Fig. 14.

Comparing experimentally determined phase compositions and the two-phase equilibria with the assessment of Kolitsch et al. [6], several discrepancies are seen. The ternary stoichiometric phase reported by Kolitsch et al. [6] as τ_3 with the composition $CeMg_3Zn_5$ ($Ce_{11.11}Mg_{33.33}Zn_{55.56}$) was found to be $Ce_{12.9\pm0.1}Mg_{29.2\pm0.9}Zn_{57.8\pm0.8}$ (Phase 4). This composition was calculated as an average from five EPMA measurements. The maximal solid solubility of the Phase 3 (reported by [6] as τ_4) was found to be at 48.3 at% Zn. The experimental results of this study also show substantial deviation from the τ_2 composition reported by ref. [6] in the three-phase region τ_4-τ_2-$(Mg,Zn)_3Ce$. The τ_2 in ref. [6] contains 35.5 at% Zn at 300 °C, while the experimental results gave 24.5 at% Zn at 350 °C. This change has been determined from the experimentally obtained tie-lines "Phase 1–Phase 3" and "Phase 1–$(Mg,Zn)_3Ce$" at 350 °C (see Table 4 and Fig. 14).

4.2. {Mg–50 at% Zn}–Ce solid–solid diffusion couple

The micrograph of the {Mg–50 at% Zn}–Ce solid–solid diffusion couple, presented in Fig. 15, contains five zones. The sample was studied via SEM/EDS and the results of quantitative EDS analysis are presented in Table 5. The diffusion path starts from the Mg–50 at% Zn binary alloy. The MgZn phase that dominates in this binary alloy is in equilibrium with the Phase 2. Phase 2 was not previously reported in the literature. Despite of the fact that the Ce concentration is only around 2 at%, this is a ternary phase. There is no binary phase at 45 at% Zn in the Mg–Zn system. The closest binary phase is MgZn that contains ~52 at% Zn. The presence of Phase 2 in other diffusion couples (see below) proves its thermodynamic stability. Because composition of the Phase 2 has very low variation in equilibria with various phases it can be concluded that it is a phase with narrow homogeneity ranges or is stoichiometric (Table 5).

Table 6
Results of EDS analysis of interdiffusion layers in the {Mg–54 at% Zn}–Ce diffusion couple.

	Ce (at%)	Mg (at%)	Zn (at%)	Comments
Zone 1	0	45.94	54.06	Mg–54 at% Zn binary alloy
Zone 2	1.66	54.2	44.14	Phase 2
Zone 3	8.79	29.25	61.94	Phase 5
Zone 4	34.44	0	65.56	$CeZn_2$
Zone 5	51.29	0	48.71	CeZn
Zone 6	100	0	0	Pure Ce

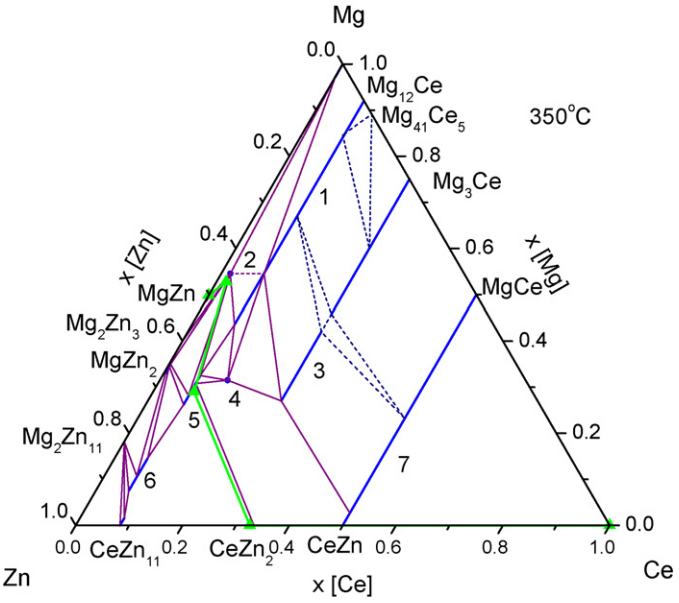

Fig. 16. {Mg–50 at% Zn}–Ce diffusion path.

The diffusion path goes from Phase 2 to Phase 5 establishing "Phase 2–Phase 5" equilibrium. Phase 5 has a composition similar to τ_3 reported by ref. [6]. The next equilibrium is between "Phase 5–$CeZn_2$", which was not previously reported. No ternary solid solubility was detected for the $CeZn_2$ phase. The $CeZn_2$ layer is in contact with pure Ce, but from the binary phase diagram it is known that the CeZn layer should be between these phases. It is believed that the CeZn layer between $CeZn_2$ and Ce was too thin and therefore under the detection limit. The diffusion path is presented in Fig. 16.

4.3. {Mg–54 at% Zn}–Ce solid–solid diffusion couple

The {Mg–54 at% Zn}–Ce solid–solid diffusion couple contains six zones. The micrograph of the sample is presented in Fig. 17. The sample was studied via SEM/EDS and the results of quantitative EDS analysis are presented in Table 6. The diffusion path starts from the Mg–54 at% Zn binary alloy. Similar to previous diffusion couple the MgZn phase dominates in Mg–54 at% Zn binary alloy and the first equilibrium is established to the Phase 2. The full diffusion path is "MgZn–Phase 2-Phase 5-$CeZn_2$-CeZn–Ce". In general

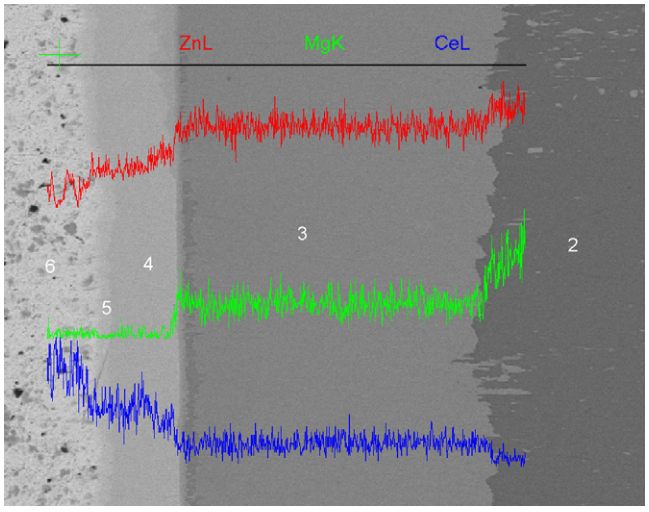

Fig. 17. {Mg–54 at% Zn}–Ce solid–solid diffusion couple.

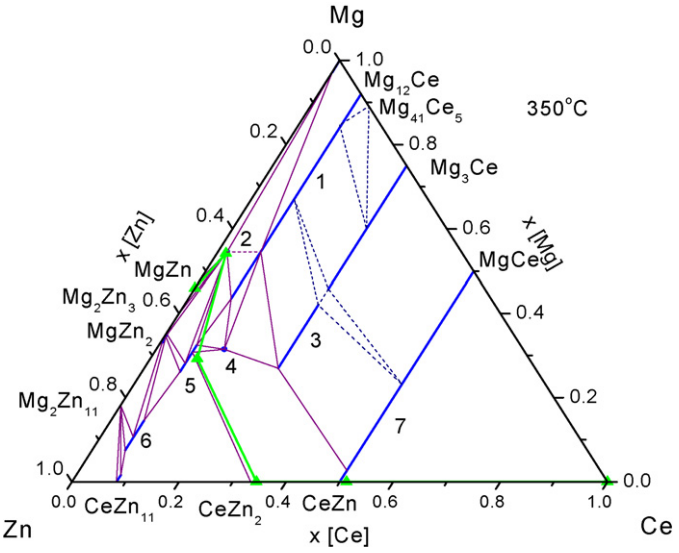

Fig. 18. {Mg–54 at% Zn}–Ce diffusion path.

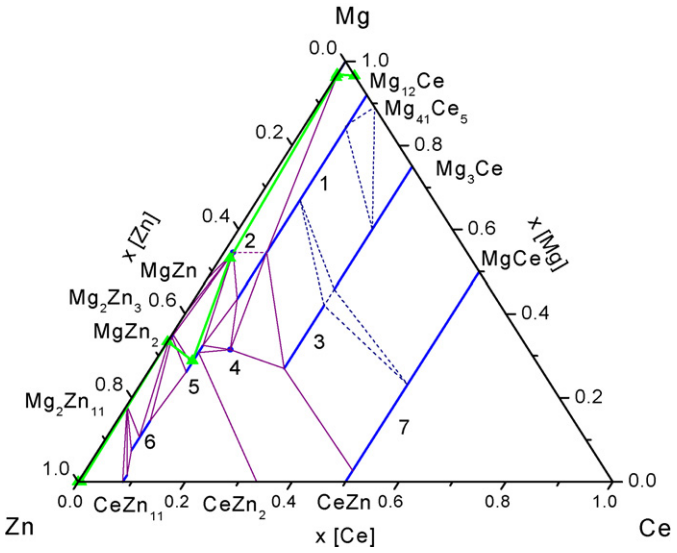

Fig. 20. {Mg–3.5 at% Ce}–Zn diffusion path.

the diffusion path of the {Mg–54 at% Zn}–Ce solid–solid diffusion couple is the same as the diffusion path of the previous {Mg–50 at% Zn}–Ce solid–solid diffusion couple. The only difference is the well established CeZn layer, but even in this sample the CeZn layer is extremely thin (see Fig. 17). The comparison of the diffusion path to the phase diagram is shown in Fig. 18.

The micrograph of the {Mg–3.5 at% Ce}–Zn solid–liquid diffusion couple is presented in Fig. 19. Because interdiffusion occurred between the solid (Mg–3.5 at% Ce) alloy and liquid Zn, no well-developed layers were formed. As illustrated in Fig. 19, several zones of two-phase equilibrium can be distinguished. The sample was studied by SEM/EDS and the phase equilibria were detected and plotted on the phase diagram as a diffusion path (see Fig. 20). The following phase equilibria were found:

- "$Mg_{12}Ce$–(Mg) solid solution" (in the (Mg–3.5 at% Ce) alloy)
- "(Mg) solid solution–Phase 2"
- "Phase 2–Phase 5"
- "Phase 5–$MgZn_2$"
- "$MgZn_2$–(Zn)".

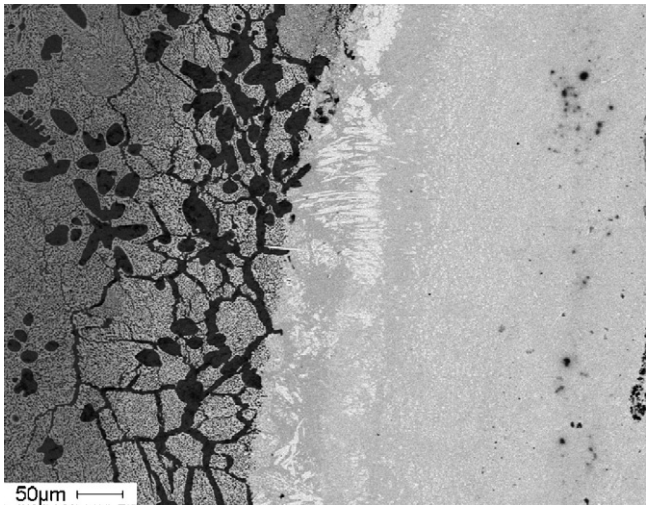

Fig. 19. {Mg–3.5 at% Ce}–Zn solid–liquid diffusion couple.

Table 7
Results of EDS analysis of interdiffusion zones in the {Mg–3.5–at% Ce}–Zn diffusion couple.

	Ce (at%)	Mg (at%)	Zn (at%)	Comments
Zone 1	3.43	96.57	0.00	Mg solid solution in Mg–3.5 at% Ce binary alloy
Zone 2	0.00	96.91	3.09	Mg solid solution
Zone 3	1.82	53.14	45.04	Phase 2
Zone 4	6.97	28.83	64.19	Phase 5
Zone 5	0.76	34.32	64.92	$MgZn_2$
Zone 6	0.52	0.00	99.49	Zn solid solution

The results of quantitative EDS analysis of the phase found in the sample are presented in Table 7. Several ternary eutectic regions were found in this sample. They were quantitatively analyzed using EDS area scan. The results of the quantitative analysis presented in Table 8 are average of at least three different regions of each eutectic. The sample micrograph of the eutectic region is presented in Fig. 21.

Similar to {Mg–3.5 at% Ce}–Zn diffusion couple, the {Mg–8.5 at% Ce}–Zn solid–liquid do not have well developed layers. Several zones of two – and three-phase equilibrium were discerned. The sample was studied by SEM/EDS and the phase equilibria were detected and plotted on the phase diagram as a diffusion path (see Fig. 22). The following phase equilibria were found:

- "$Mg_{12}Ce$–$Mg_{41}Ce_5$" (in the (Mg–8.5 at% Ce) alloy)
- "$(Mg,Zn)_{12}Ce$ solid solution–Phase 5"
- "Phase 5–Phase 2"
- "Phase 5–$MgZn_2$"
- "$MgZn_2$–Phase 6"
- "Phase 6–Mg_2Zn_{11}"

Table 8
Results of EDS analysis of eutectic regions in the {Mg–3.5 at% Ce}–Zn diffusion couple.

	Ce (at%)	Mg (at%)	Zn (at%)
Eutectic 1	4.89	95.11	0.00
Eutectic 2	4.94	92.50	2.57
Eutectic 3	4.04	89.90	6.05
Eutectic 4	5.06	69.50	25.45
Eutectic 5	3.89	32.39	63.72
Eutectic 6	3.89	43.14	52.97
Eutectic 7	1.98	33.09	64.94

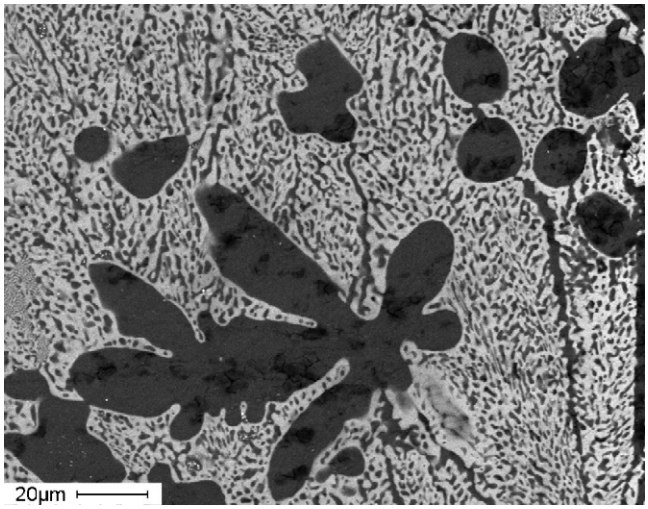

Fig. 21. The sample micrograph of the eutectic region in the{ Mg–3.5 at% Ce }–Zn diffusion couple.

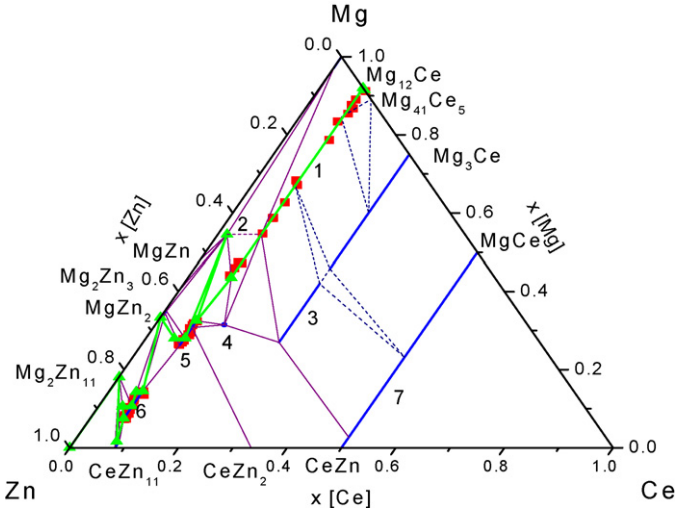

Fig. 22. {Mg–8.5 at% Ce}–Zn diffusion path.

- "Phase 6–$CeZn_{11}$"
- "Mg_2Zn_{11}–$CeZn_{11}$".

The analysis of the single phase regions showed that phases 1, 5 and 6 have wide ranges of homogeneity. The experimentally determined boundaries of these solid solutions by EDS and EPMA are presented in Table 9. The line scan of the $(Mg,Zn)_{12}Ce$ solid solution area presented in Fig. 23 demonstrates a substantial variation of the Mg and Zn concentrations with a constant Ce content.

To determine the extent of the $(Mg,Zn)_{12}Ce$ solid solution, several EDS point measurements were made along the scanning line.

Table 9
Results of EDS and EPMA analysis of solid solutions in the {Mg–8.5 at% Ce}–Zn diffusion couple.

	Ce (at%)	Mg (at%)	Zn (at%)	Comments
Start	8.04	91.96	0.00	$Mg_{12}Ce$ solid solution
End	8.04	43.47	48.49	
Start	7.10	32.47	60.43	Phase 5
End	7.10	26.24	66.66	
Start	6.21	14.56	79.23	Phase 6
End	6.21	7.52	86.27	

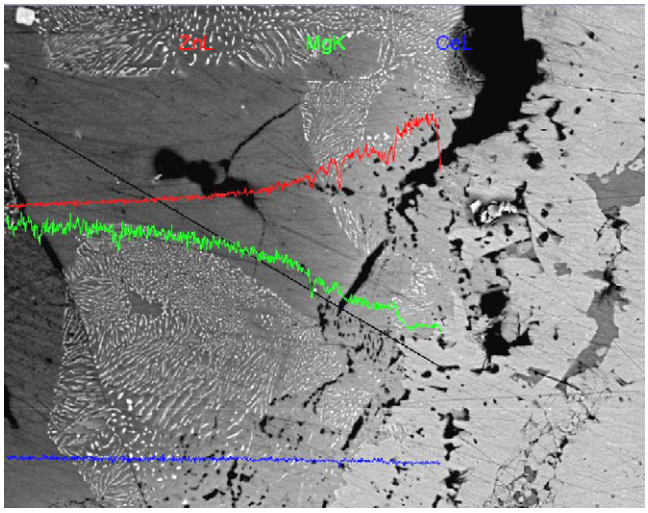

Fig. 23. The micrograph of the line scan of $Mg_{12}Ce$ phase in the {Mg–8.5 at% Ce}–Zn diffusion couple.

The results of the EDS analysis are shown as red squares on Fig. 22. The extension of the binary $Mg_{12}Ce$ solid solution determined by EDS was found to be 48.49 at% Zn. In contrast, Kolitsch et al. [6] separate this solid solution on $Mg_{12}Ce$ that dissolves ~6 at% Zn and τ_2 phase with different Ce content. The careful analysis of the line scan has shown no sharp deviation of the Ce content. As could be seen in Fig. 23, the concentration of Ce is represented by the straight line. At the same time the Mg concentration is monotonically decreasing, while the Zn concentration is monotonically increasing up to be 48.49 at% Zn. The variations of Mg and Zn concentrations on the line scan correspond to the porosities on the micrograph and therefore could be neglected. All these results point to the conclusion that the τ_2 phase reported by Kolitsch et al. [6] is a part of the $Mg_{12}Ce$ solid solution that dissolves up to 48.49 at% Zn. To check the EDS results, point analysis of the $Mg_{12}Ce$ solid solution region was performed using EPMA. The results of the EPMA point analysis proved that content of Ce along the entire $Mg_{12}Ce$ region is constant within the error of measurement which supported the above conclusion. A similar situation could appear for the Phase 3 and Mg_3Ce solid solution. According to Kolitsch et al. [6], only a small two-phase

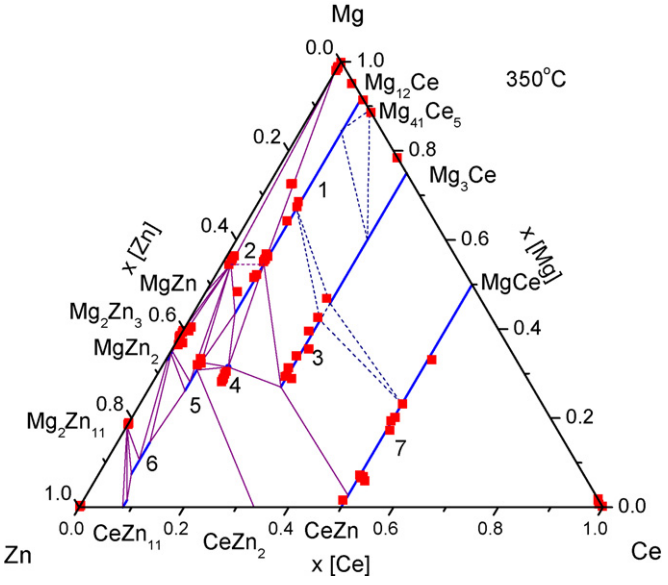

Fig. 24. Phase composition obtained by EPMA.

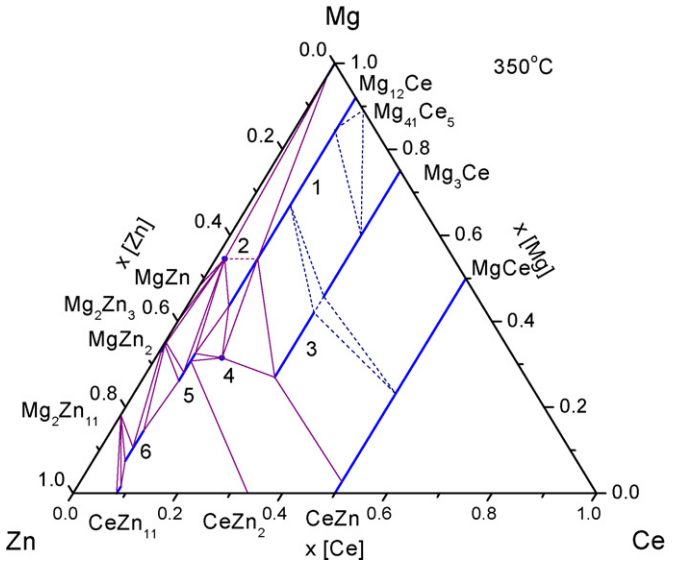

Fig. 25. Partial isothermal section of the Mg–Ce–Zn system at 350 °C constructed using experimental data from the diffusion couple study.

Table 10
Results of EDS and EPMA analysis of binary phases in the {Mg–8.5 at% Ce}–Zn diffusion couple.

	Ce (at%)	Mg (at%)	Zn (at%)	Comments
Phase A	8.54	91.46	0	$Mg_{12}Ce$ in binary alloy
Phase B	0.375	33.838	65.788	$MgZn_2$
Phase C	0.087	18.133	81.782	Mg_2Zn_{11}
Phase D	7.873	1.575	90.550	$CeZn_{11}$

region divides the Mg_3Ce solid solution and the Phase 3 denoted by Kolitsch as τ_4. By analogy to the τ_2 phase, the Phase 3 (τ_4 phase) could be a part of the Mg_3Ce solid solution. However, since there is no experimental evidence of this fact, the existence of the two phase region reported Kolitsch et al. [6] is accepted. Due to the 50 °C temperature difference between the isothermal section studied by Kolitsch et al. [6] and the present work, the location of this two-phase field cannot be determined with certainty and, therefore, it is shown as a dotted line in Figs. 7–25.

Four binary phases (A–D) were found in the {Mg–8.5 at% Ce}–Zn diffusion couple. Their compositions detected using EDS and EPMA are presented in Table 10. To check the quality of the EDS analysis, EPMA measurements of the key phases were carried out. The concentrations obtained by EDS analysis have a good agreement with the EPMA measurements. The compositions of the phases measured by EPMA are presented in Fig. 24.

5. Conclusions

The partial isothermal section of the Ce–Mg–Zn system at 350 °C was constructed using diffusion couple technique and illustrated in Fig. 25. Two new ternary phases (Phases 2 and 6) were found. Solid solubilities of binary and ternary solid solutions were determined using EDS and EPMA techniques. The phase equilibria completely determined in the Mg-rich corner of the Ce–Mg–Zn system at 350 °C.

Acknowledgements

This work was supported by Natural Sciences and Engineering Research Council (NSERC) of Canada, General Motors of Canada and McGill University, Faculty of Engineering. Pierre Vermette of McGill University is gratefully acknowledged for assistance in the preparation of the diffusion couples.

References

[1] A.A. Nayeb-Hashemi, J.B. Clark, in: T.B. Massalski, H. Okamoto, P.R. Subramanian, L. Kacprzak (Eds.), Binary Alloy Phase Diagrams, second ed., ASM International, Materials Park, Ohio, 1990, pp. 1077–1080.
[2] X. Zhang, D. Kevorkov, M.O. Pekguleryuz, in: A. Luo, N. Neelameggham, R. Beals (Eds.), Magnesium Technology, TMS, Warrendale, PA, USA, 2006, pp. 441–444.
[3] B. Predel (Ed.), Phase Equilibria, Crystallographic and Thermodynamic Data of Binary Alloys, Lnadolt-Bornstein, Group IV, Physical Chemistry, 5 Springer-Verlag, Berlin, Germany, 1998.
[4] J.B. Clark, L. Zabdyr, Z. Moser, in: T.B. Massalski, H. Okamoto, P.R. Subramanian, L. Kacprzak (Eds.), Binary Alloy Phase Diagrams, second ed., ASM International, Materials Park, Ohio, 1990, pp. 2571–2572.
[5] T.B. Massalski, in: T.B. Massalski, H. Okamoto, P.R. Subramanian, L. Kacprzak (Eds.), Binary Alloy Phase Diagrams, second ed., ASM International, Materials Park, Ohio, 1990, pp. 1132–1133.
[6] U. Kolitsch, P. Bellen, S. Kaesche, D. Maccio, N. Bochvar, Y. Liberov, P. Rogl, in: G. Effenberg, G. Petzow (Eds.), Cerium–Magnesium–Zinc, in Ternary Alloys – A Comprehensive Compendium of Evaluated Constitutional Data and Phase Diagrams, VCH Verlagsgesellscahft, MSI GmbH, Weinheim, Stuttgart, Germany, 2000, pp. 168–176.
[7] A.M. Korolkov, Y.P. Saldau, Izv. Sekt. Fiziko-Khimich Analiza Akad. Nauk SSSR. 16 (2) (1946) 295–306.
[8] E.V. Melnik, O.F. Zmii, E.E. Cherkasim, Vestn. L'viv. Univ. Ser. Khim. 19 (1977) 34–36.
[9] E.V. Melnik, M.F. Kostina, Ya.P.Yarmlyuk, O.F. Zmii, in: Mater. Vses. Soveshch. Issled. Razrab, Primen, Magnievyhk Splavov, 1978, pp. 95–99.
[10] M.E. Drits, E.I. Drozdova, I.G. Krol'kova, V.V. Kinzhibalo, A.T. Tyvanchuk, Russ. Met. 2 (1989) 195–197.